Non-local Andreev reflection in superconducting quantum dots

Dmitri S. Golubev and Andrei D. Zaikin

Forschungszentrum Karlsruhe, Institut für Nanotechnologie, 76021, Karlsruhe, Germany and
I.E. Tamm Department of Theoretical Physics, P.N. Lebedev Physics Institute, 119991 Moscow, Russia

With the aid of the Keldysh technique we develop a microscopic theory of non-local electron transport in three-terminal NSN structures consisting of a chaotic superconducting quantum dot attached to one superconducting and two normal electrodes. Our theory fully accounts for non-equilibrium effects and disorder in a superconducting terminal. We go beyond perturbation theory in tunneling and derive a general expression for the system conductance matrix which remains valid in both weak and strong tunneling limits. We demonstrate that the proximity effect yields a decrease of crossed Andreev reflection (CAR). Beyond weak tunneling limit the contribution of CAR to the non-local conductance does not cancel that of direct electron transfer between two normal terminals. We argue that temperature dependence of the non-local resistance of NSN devices is determined by the two competing processes – Andreev reflection and charge imbalance – and it has a pronounced peak occurring at the crossover between these two processes. This behavior is in a good agreement with recent experimental observations.

I. INTRODUCTION

Non-local (crossed) Andreev reflection[1,2] is the process which occurs in multi-terminal hybrid normal metal-superconductor-normal metal (NSN) proximity structures and involves two subgap electrons entering a superconductor from two *different* normal terminals and forming a Cooper pair there. This is in contrast to the standard mechanism of (local) Andreev reflection[3] (AR) in which case two subgap electrons enter a superconductor from the same normal electrode through the same interface. The phenomenon of crossed Andreev reflection (CAR) manifests itself, e.g., in the dependence of the current I_L through the left NS interface of an NSN structure on the voltage V_R across the right NS interface. As a result, the non-local conductance $G_{LR} = \partial I_L/\partial V_R$ of an NSN device differs from zero and can be detected experimentally. Such experiments have recently been performed by several groups[4,5,6] providing a number of interesting observations some of which remain not fully understood.

It is important to mention that CAR is not the only process which contributes to the non-local conductance G_{LR}. Another relevant process is direct electron transfer (DET) between two normal terminals through the super-conductor. In the tunneling limit this process is nothing but the so-called elastic cotunneling (EC). It turned out[7] that in the lowest order in tunneling the contributions from EC and CAR to G_{LR} exactly cancel each other in the limit of low temperatures and voltages, i.e. the non-local conductance G_{LR} should vanish in this limit.

Note that this result[7] is applicable only provided transmissions of both NS interfaces remain small which is not always the case in the experiments. At higher transmissions processes to all orders should be taken into account and the contributions of DET and CAR do not anymore cancel each other. Hence, G_{LR} does not vanish beyond the tunneling limit. In the case of ballistic electrodes a non-perturbative (in barrier transmissions) theory was recently developed by Kalenkov and one of the authors[8,9].

This theory allowed to study the non-local conductance of NSN devices at arbitrary transmissions leading to a conclusion that CAR contribution to G_{LR} *vanishes* in the limit of fully open NS barriers. This result might seem counterintuitive since ordinary (local) AR reaches its maximum at full barrier transmissions. In contrast, CAR is essentially a non-local effect which requires "mixing" of trajectories for electrons going between two normal terminals with those for electrons going deep into a superconductor and describing the flow of Cooper pairs out of the contact area. Provided there exists no normal electron reflection at both NS interfaces such mixing does not occur, CAR vanishes and the only remaining contribution to G_{LR} in this case is one from DET.

For completeness, let us point out that the exact cancellation between EC and CAR contributions[7] can also be violated by other means. One of them is simply to lift the spin degeneracy in the system. This can be achieved, e.g., by considering NSN structures with spin-active interfaces[9] or by using ferromagnets (F) as normal metallic electrodes[10,11,12]. Experiments with FSF structures[4] directly demonstrated the dependence of the non-local conductance G_{LR} on the polarization of F-electrodes.

Yet another way to avoid the cancellation between EC and CAR terms already in the tunneling limit is to include interactions. This idea has been put forward in Ref. 13. The effect of electron-electron interactions on non-local conductance of NSN devices – in particular in the presence of disorder – is an interesting issue to be investigated further. Such investigation is, however, beyond the scope of the present paper. Here we only want to point out that interactions are not very likely to play the dominant role in the experiments[4,5,6]. This is because typical resistances involved in these experiments were rather low and the corresponding dimensionless conductances strongly exceeded unity. Under such conditions the effect of Coulomb interactions on AR is weak[14,15,16] and a similar situation with EC and CAR can be expected. In general, however, the combined effect of electron-electron

interactions and disorder on non-local properties of NSN devices can be important.

In the absence of Coulomb interaction the effect of disorder on non-local electron transport in NSN was recently considered in Refs. 17,18,19. Brinkman and Golubov[17] employed the quasiclassical formalism of Usadel equations and proceeded perturbatively in the interface transmissions. They found that the proximity effect in the normal electrodes in combination with disorder can strongly enhance both EC and CAR contributions to the non-local conductance. Duhot and Melin[19] argued that weak-localization-type of effects inside the superconductor may influence non-local electron transport in NSN structures. Morten *et al.*[18] considered a device with normal terminals attached to a superconductor via an additional *normal* island (dot) and analyzed this structure within the framework of the circuit theory. In this paper we will extend and generalize this model by considering a *superconducting* dot attached to one superconducting and two normal terminals as shown in Fig. 1.

Our main goal is to study the combined effect of proximity and disorder *inside* the superconductor (dot). In addition, as it was demonstrated in experiments[4,6], non-equilibrium effects, such as charge imbalance, inside a superconducting electrode may play a significant role. These effects will be included into our consideration too. We are going to show that the "peaked" temperature dependence of the non-local resistance R_{LR} observed in the experiments[4,6] can be explained as a result of the competition between charge imbalance and Andreev reflection. The crossover temperature between these two processes T^* (defined in Eq. (65) below) sets the position of the maximum in the dependence $R_{LR}(T)$.

In order to illustrate the main idea of our approach let us recall that the exact cancellation between EC and CAR terms[7] occurs only at energies below the superconducting gap while at higher energies (or in the normal state) CAR vanishes and EC remains the only relevant mechanism of electron transport. It is clear, therefore, that including the proximity effect due to the presence of normal electrodes immediately yields non-zero sub-gap density of states inside the supercoducting electrode which in turn should yield a decrease of CAR, thus eliminating its compensation by EC and leaving the non-local conductance G_{LR} non-zero. This is precisely what we find. In order to correctly account for the above effects it is necessary to proceed non-perturbatively in tunneling and consider interface conductances exceeding unity. Under these conditions the concept of elastic cotunneling becomes irrelevant and it would be more appropriate to speak about direct electron transfer between two N-electrodes which includes processes of all orders in the interface transmissions.

The structure of our paper is as follows. In Sec. 2 we will introduce our model and outline the formalism to be used below. In Sec. 3 we will evaluate the Green-Keldysh functions of our system which will be used in Sec. 4 in order to derive the general expressions for the
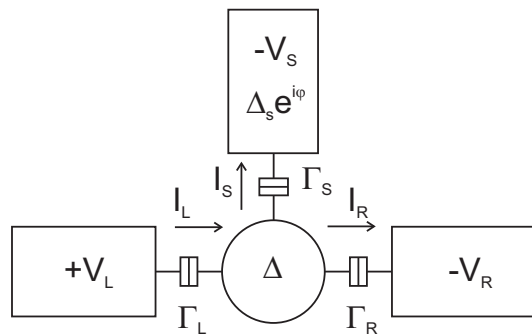

FIG. 1: Superconducting quantum dot coupled to two normal and one superconducting leads.

non-local currents in our NSN device. In the limit of low bias voltages these general results are further analyzed in details in Sec. 5 where we also illustrate their relation to previous theoretical works and to experimental findings[4,6].

II. THE MODEL AND BASIC FORMALISM

Below we will consider a chaotic superconducting quantum dot with the mean level spacing δ connected to one superconducting (S) and two normal (L and R) massive electrodes by means of tunnel barriers. This structure is schematically shown in Fig. 1. The typical size of the dot d is supposed to be sufficiently small, $d \lesssim \xi_0$, where ξ_0 is the superconducting coherence length. Although we assume the channel transmissions of all three junctions are small, $T_n^{(j)} \ll 1$ (here and below $j = S, L, R$), their dimensionless conductances $g_j = 2\sum_n T_n^{(j)}$ can take any (large) value provided the number of conducting channels is sufficiently large. The magnitudes of the superconducting order parameters in the dot and the electrode S are denoted respectively as Δ and Δ_S. The phase difference across the Josephson junction between the dot and the S-electrode is denoted by φ.

Let us introduce the electron escape rate through the j-th junction $\Gamma_j = g_j \delta / 4\pi$. Below we will demonstrate that transport properties of our system essentially depend on the parameters Γ_j / Δ. Our theoretical approach allows to obtain the exact solution of our problem applicable for all values of Γ_j / Δ.

The Hamiltonian of our system reads

$$H = H_{qd} + H_L + H_R + H_S + H_{TL} + H_{TR} + H_{TS}, \quad (1)$$

where

$$H_{qd} = \sum_{n,\,\alpha=\uparrow,\downarrow} \xi_n \hat{d}^\dagger_{\alpha n} \hat{d}_{\alpha n} + \sum_n \left(\Delta \hat{d}^\dagger_{\uparrow n} \hat{d}^\dagger_{\downarrow,-n} + \text{c.c.} \right) \quad (2)$$

is the Hamiltonian of an isolated quantum dot,

$$H_{L,R} = \sum_{k,\alpha} \epsilon_{k\alpha} \hat{c}^\dagger_{k\alpha;L,R} \hat{c}_{k\alpha;L,R} \quad (3)$$

represent the Hamiltonians of the left and right normal leads,

$$H_S = \sum_{k,\alpha} \epsilon_{k\alpha} \hat{c}_{k\alpha;S}^\dagger \hat{c}_{k\alpha;S} + \sum_k \left(\Delta_S \hat{c}_{\uparrow,k,S}^\dagger \hat{c}_{\downarrow,-k,S}^\dagger + \text{c.c.} \right)$$
(4)

is the Hamiltonian of the massive superconducting electrode and

$$H_{Tj} = \sum_{nk,\alpha} \left(t_{nk,j} \hat{d}_{n\alpha}^\dagger \hat{c}_{k\alpha;j} + t_{nk,j}^* \hat{c}_{k\alpha;j}^\dagger \hat{d}_{n\alpha} \right)$$
(5)

define the tunneling Hamiltonians for the junctions $j = S, L, R$.

Employing the Keldysh formalism we define non-equilibrium 4×4 Green-Kedysh function of n-th energy level in the quantum dot:

$$\check{G}_n = \begin{pmatrix} \hat{G}_n & \hat{F}_n \\ \hat{F}_n^\dagger & \hat{G}_n^\dagger \end{pmatrix},$$
(6)

where

$$\hat{G}_n = -i \begin{pmatrix} \langle \mathcal{T} \hat{d}_{\uparrow n}(t_1) \hat{d}_{\uparrow n}^\dagger(t_2) \rangle & -\langle \hat{d}_{\uparrow n}^\dagger(t_2) \hat{d}_{\uparrow n}(t_1) \rangle \\ \langle \hat{d}_{\uparrow n}(t_1) \hat{d}_{\uparrow n}^\dagger(t_2) \rangle & \langle \mathcal{T}^{-1} \hat{d}_{\uparrow n}(t_1) \hat{d}_{\uparrow n}^\dagger(t_2) \rangle \end{pmatrix},$$

$$\hat{G}_n^\dagger = -i \begin{pmatrix} \langle \mathcal{T} \hat{d}_{\downarrow n}^\dagger(t_1) \hat{d}_{\downarrow n}(t_2) \rangle & -\langle \hat{d}_{\downarrow n}(t_2) \hat{d}_{\downarrow n}^\dagger(t_1) \rangle \\ \langle \hat{d}_{\downarrow n}^\dagger(t_1) \hat{d}_{\downarrow n}(t_2) \rangle & \langle \mathcal{T}^{-1} \hat{d}_{\downarrow n}^\dagger(t_1) \hat{d}_{\downarrow n}(t_2) \rangle \end{pmatrix},$$

$$\hat{F}_n = -i \begin{pmatrix} \langle \mathcal{T} \hat{d}_{\uparrow n}(t_1) \hat{d}_{\downarrow n}(t_2) \rangle & -\langle \hat{d}_{\downarrow n}(t_2) \hat{d}_{\uparrow n}(t_1) \rangle \\ \langle \hat{d}_{\uparrow n}(t_1) \hat{d}_{\downarrow n}(t_2) \rangle & \langle \mathcal{T}^{-1} \hat{d}_{\uparrow n}(t_1) \hat{d}_{\downarrow n}(t_2) \rangle \end{pmatrix},$$

$$\hat{F}_n^\dagger = -i \begin{pmatrix} \langle \mathcal{T} \hat{d}_{\downarrow n}^\dagger(t_1) \hat{d}_{\uparrow n}^\dagger(t_2) \rangle & -\langle \hat{d}_{\uparrow n}^\dagger(t_2) \hat{d}_{\downarrow n}^\dagger(t_1) \rangle \\ \langle \hat{d}_{\downarrow n}^\dagger(t_1) \hat{d}_{\uparrow n}^\dagger(t_2) \rangle & \langle \mathcal{T}^{-1} \hat{d}_{\downarrow n}^\dagger(t_1) \hat{d}_{\uparrow n}^\dagger(t_2) \rangle \end{pmatrix}.$$

Note that here we do not introduce the off-diagonal elements of the Green function $\check{G}_{nm}$. In the next section we will demonstrate that these off-diagonal elements vanish, $\check{G}_{nm} = 0$ for $n \neq m$, provided the dot is fully chaotic and all channel transmissions are small, $T_n^{(j)} \ll 1$. The Green functions of the leads are defined analogously.

The current through the left tunnel junction is expressed as

$$I_L = \frac{e}{2} \sum_{nk} |t_{nk}|^2 \int \frac{dE}{2\pi} \text{tr} \left[\check{G}_n(E) \check{\Lambda} \check{G}_{k,L}(E) \right.$$
$$\left. - \check{G}_{k,L}(E) \check{\Lambda} \check{G}_n(E) \right].$$
(7)

Here Λ is the 4×4 diagonal matrix with the matrix elements $\Lambda_{11} = -1$, $\Lambda_{22} = 1$, $\Lambda_{33} = 1$ and $\Lambda_{44} = -1$. The functions $\check{G}_n(E)$ and $\check{G}_L(E)$ are the Fourier components of the Green-Keldysh functions for the dot and the left lead respectively. The currents across the right junction and across the Josephson junction between the dot and the superconducting electrode are defined analogously.

In our subsequent calculation we will make use of the fact that coupling of the n-th energy level of a chaotic dot to the leads does not depend on the number n, i.e. it remains the same for all levels. Hence, the effective level width $\delta\epsilon = \Gamma_L + \Gamma_R + \Gamma_S$ is also the same for all the dot levels. This observation enables us to first evaluate the 4×4 Green-Keldysh functions for each single energy level, then calculate its contribution to the current and afterwards perform a summation over all energy levels. This program will be accomplished below.

III. GREEN-KELDYSH FUNCTIONS

The Green-Keldysh functions of the dot $\check{G}_{ln}$ obey the Dyson equation

$$\sum_l \left[\check{G}_{n,qd}^{-1} \delta_{ml} - \check{\Sigma}_L^{ml} - \check{\Sigma}_R^{ml} - \check{\Sigma}_S^{ml} \right] \check{G}_{ln} = \check{1} \delta_{mn},$$
(8)

where

$$\check{G}_{n,qd}^{-1} = \begin{pmatrix} E - \xi_n & 0 & -\Delta & 0 \\ 0 & -E + \xi_n & 0 & \Delta \\ -\Delta & 0 & E + \xi_n & 0 \\ 0 & \Delta & 0 & -E - \xi_n \end{pmatrix},$$
(9)

and

$$\check{\Sigma}_j^{mn} = \sum_k t_{km,j}^* t_{kn,j} \check{\Lambda} \check{G}_{k,j}(E) \check{\Lambda}.$$
(10)

is the self-energy of the j−th junction.

In a chaotic quantum dot off-diagonal matrix elements of any operator between the m−th and the n−th energy levels tend to zero provided their energies are not too far from each other, $|\xi_n - \xi_m| \lesssim D/d^2$, where D is the diffusion coefficient for electrons inside the dot[20]. In addition, under these conditions the diagonal matrix elements do not depend on the level number n, i.e. $\langle n|\hat{A}|n \rangle = \text{const}$[20]. Hence, we obtain

$$\check{\Sigma}_j^{mn} = \delta_{mn} \check{\Sigma}_j,$$
(11)

where

$$\check{\Sigma}_j = |t_j|^2 \check{\Lambda} \sum_k \check{G}_{k,j}(E) \check{\Lambda}.$$
(12)

Then the Dyson equation for the Green-Keldysh function acquires the form

$$\left[\check{G}_{n,qd}^{-1} - \check{\Sigma}_L - \check{\Sigma}_R - \check{\Sigma}_S \right] \check{G}_n = \check{1}.$$
(13)

Performing the summation over k in Eq. (12) with the known expressions for the Green-Keldysh functions of the leads is straightforward. As a result, the self-energies for the junctions between the dot and the normal leads take the form

$$\check{\Sigma}_{L,R} = \frac{\Gamma_{L,R}}{2i} \begin{pmatrix} \hat{\sigma}_z \hat{Q}(E \pm eV_{L,R}) & 0 \\ 0 & \hat{\sigma}_z \hat{Q}(E \mp eV_{L,R}) \end{pmatrix}$$
(14)

where $\hat{\sigma}_z$ is the Pauli matrix and $\hat{Q}$ is the 2×2 matrix which reads

$$\hat{Q}(E) = \begin{pmatrix} 1 - 2n(E) & 2n(E) \\ 2 - 2n(E) & -1 + 2n(E) \end{pmatrix}. \tag{15}$$

Here $n(E) = 1/(1 + e^{E/T})$ is the Fermi function.

The self-energy $\check{\Sigma}_S$ for the Josephson junction between the dot and the S-electrode, though somewhat more involved, is evaluated analogously. Combining the resulting expression for $\check{\Sigma}_S$ with Eq. (14) we obtain

$$\check{\Sigma} = \check{\Sigma}_L + \check{\Sigma}_R + \check{\Sigma}_S$$
$$= -\frac{\Gamma_S F_S(E)}{2} \begin{pmatrix} E/\Delta_S & -e^{i\varphi} \\ -e^{-i\varphi} & E/\Delta_S \end{pmatrix} \otimes \hat{\sigma}_z$$
$$- i\frac{\Gamma(E)}{2} \begin{pmatrix} 1 & 0 \\ 0 & 0 \end{pmatrix} \otimes \hat{\sigma}_z \hat{Q}_{qd}(E)$$
$$- i\frac{\Gamma(E)}{2} \begin{pmatrix} 0 & 0 \\ 0 & 1 \end{pmatrix} \otimes \hat{\sigma}_z \hat{Q}'_{qd}(E)$$
$$+ i\frac{\Gamma_S}{2} \frac{\Delta_S N_S(E)}{E} \begin{pmatrix} 0 & e^{i\varphi} \\ e^{-i\varphi} & 0 \end{pmatrix} \otimes \hat{\sigma}_z \hat{Q}_S(E), \tag{16}$$

where we denoted $F_S(E) = \frac{\Delta_S \theta(\Delta_S - |E|)}{\sqrt{\Delta_S^2 - E^2}}$, introduced the density of states in the superconductor $N_S(E) = \frac{|E| \theta(|E| - \Delta_S)}{\sqrt{E^2 - \Delta^2}}$ and defined

$$\Gamma(E) = \Gamma_L + \Gamma_R + \Gamma_S N_S(E), \tag{17}$$

as the total escape rate of an electron from the dot through all three barriers. The $\hat{Q}$-matrices in Eq. (16) read

$$\hat{Q}_{qd} = \begin{pmatrix} 1 - 2n_{qd} & 2n_{qd} \\ 2 - 2n_{qd} & -1 + 2n_{qd} \end{pmatrix}, \tag{18}$$

where

$$n_{qd}(E) = \frac{\Gamma_L}{\Gamma(E)} n(E + eV_L) + \frac{\Gamma_R}{\Gamma(E)} n(E - eV_R)$$
$$+ \frac{\Gamma_S}{2\Gamma(E)} \big(N_S(E) + \theta(|E| - \Delta_S)\big) n(E - eV_S)$$
$$+ \frac{\Gamma_S}{2\Gamma(E)} \big(N_S(E) - \theta(|E| - \Delta_S)\big) n(E + eV_S) \tag{19}$$

is the distribution function in the quantum dot,

$$\hat{Q}'_{qd}(E, V_L, V_R, V_S) = \hat{Q}_{qd}(E, -V_L, -V_R, -V_S) \tag{20}$$

and

$$\hat{Q}_S(E) = \big[\hat{Q}(E - eV_S) + \hat{Q}(E + eV_S)\big]/2. \tag{21}$$

We are now in a position to evaluate the Green-Keldysh function with the aid of the Dyson equation (13). The derivation is facilitated by the normalization condition for the $\hat{Q}$-matrices, $\hat{Q}^2 = 1$, as well as by the property

$$\hat{Q}_i \hat{Q}_j = \hat{1} - \hat{Q}_i + \hat{Q}_j.$$

After some algebra we finally arrive at the following expression for the dot Green-Keldysh function:

$$\check{G}_n(E, \xi_n) = \frac{1}{2} \left(\tilde{G}_n^R + \tilde{G}_n^A \right) \otimes \hat{\sigma}_z$$
$$+ i\frac{\Gamma_S N_S(E) \Delta_S}{2E} \tilde{G}_n^R \begin{pmatrix} 0 & e^{i\varphi} \\ e^{-i\varphi} & 0 \end{pmatrix} \tilde{G}_n^A \otimes \hat{Q}_S(E) \hat{\sigma}_z$$
$$- i\frac{\Gamma(E)}{2} \tilde{G}_n^R \begin{pmatrix} 1 & 0 \\ 0 & 0 \end{pmatrix} \tilde{G}_n^A \otimes \hat{Q}_{qd}(E) \hat{\sigma}_z$$
$$- i\frac{\Gamma(E)}{2} \tilde{G}_n^R \begin{pmatrix} 0 & 0 \\ 0 & 1 \end{pmatrix} \tilde{G}_n^A \otimes \hat{Q}'_{qd}(E) \hat{\sigma}_z. \tag{22}$$

Here we defined the 2×2 matrix retarded and advanced Green functions

$$\tilde{G}_n^{R,A}(E, \xi_n, \varphi) = \begin{pmatrix} G_{R,A}(E, \xi_n, \varphi) & F_{R,A}(E, \xi_n, \varphi) \\ F_{R,A}(E, \xi_n, -\varphi) & G_{R,A}(E, -\xi_n, \varphi) \end{pmatrix},$$

where

$$G_{R,A}(E, \xi, \varphi) = \frac{E + \xi + \frac{\Gamma_S F_S(E) E}{2\Delta_S} \pm i\frac{\Gamma(E)}{2}}{P_{R,A}(E, \xi, \varphi)}, \tag{23}$$

$$F_{R,A}(E, \xi, \varphi) = \frac{\Delta + \frac{\Gamma_S e^{i\varphi}}{2} \left(F_S(E) \pm i\frac{N_S(E)\Delta_S}{E} \right)}{P_{R,A}(E, \xi, \varphi)} \tag{24}$$

are respectively the normal and anomalous retarded and advanced Green functions of the superconducting quantum dot and

$$P_{R,A}(E, \xi, \varphi) = \left(E + \frac{\Gamma_S F_S(E) E}{2\Delta_S} \pm i\frac{\Gamma(E)}{2} \right)^2$$
$$- \xi^2 - \left(\Delta + \frac{\Gamma_S e^{i\varphi}}{2} \left(F_S(E) \pm i\frac{N_S(E)\Delta_S}{E} \right) \right)$$
$$\times \left(\Delta + \frac{\Gamma_S e^{-i\varphi}}{2} \left(F_S(E) \pm i\frac{N_S(E)\Delta_S}{E} \right) \right). \tag{25}$$

One can easily verify that the retarded and advanced Green functions are linked to each other by the standard relations $G_A(E, \xi, \varphi) = G_R^*(E, \xi, \varphi)$ and $F_A(E, \xi, \varphi) = F_R^*(E, \xi, -\varphi)$.

For completeness, we also present the self-consistency equation which controls the magnitude of the order parameter in the dot:

$$\Delta = -\frac{\lambda \Gamma_S}{2\delta} \sum_n \int \frac{dE}{2\pi} F_S(E) \operatorname{sign} E$$
$$\times \big[1 - n(E + eV_S) - n(E - eV_S) \big]$$
$$\times \big[\cos 2\varphi \, G_R(E, \xi_n, \varphi) G_R^*(E, -\xi_n, \varphi)$$
$$+ F_R(E, \xi_n, \varphi) F_R^*(E, \xi_n, -\varphi) \big]$$
$$+ \frac{\lambda}{\delta} \sum_n \int \frac{dE}{2\pi} \Gamma(E) \operatorname{Re} \big[e^{i\varphi} G_R(E, \xi_n, \varphi)$$
$$\times F_R^*(E, \xi_n, -\varphi) \big] \big[1 - 2n_{qd}(E) \big]. \tag{26}$$

where λ is the BCS coupling constant. In general, the superconducting order parameter inside the dot should

be determined self-consistently with the aid of Eq. (26). Here we avoid this complication and set Δ equal to a constant. This assumption is justified if, for instance, the coupling between the dot and the superconducting lead is much stronger than that between the dot and the normal leads, $\Gamma_S \gg \Gamma_L, \Gamma_R$. If, in addition, we assume that both the dot and the superconducting lead are made of the same material, it would be appropriate to set $\Delta = \Delta_S$ at all temperatures and sufficiently low bias voltages.

IV. NON-LOCAL CURRENTS

We now make use of the above general results and evaluate the currents across both NS interfaces of our device. Combining Eqs. (7) and (12) we express the current across the left interface in the form

$$I_L = \frac{e}{2} \sum_n \int \frac{dE}{2\pi} \, \text{tr} \left([\check{\Sigma}_L(E), \check{\Lambda}] \check{G}_n(E) \right). \quad (27)$$

An analogous formula is obtained for the current in the right junction I_R. Substituting the results for the Green functions and self-energies derived in the previous section into the above expressions for the currents and setting $V_S = 0$, we obtain

$$I_L = I_{LS}(V_L) + \left(2\frac{\Gamma_L}{\Gamma_R} + 1 \right) I_{CAR}(V_L) + I_{DET}(V_L)$$
$$+ I_{DET}(V_R) - I_{CAR}(V_R), \quad (28)$$

$$I_R = I_{RS}(V_R) + \left(2\frac{\Gamma_R}{\Gamma_L} + 1 \right) I_{CAR}(V_R) + I_{DET}(V_R)$$
$$+ I_{DET}(V_L) - I_{CAR}(V_L), \quad (29)$$

where we defined

$$I_{LS}(V) = \frac{e\Gamma_L\Gamma_S}{\pi} \sum_n \int dE N_S(E)$$
$$\times \left\{ |G_R(E, \xi_n, \varphi)|^2 + |F_R(E, \xi_n, \varphi)|^2 \right.$$
$$\left. - \frac{2\Delta_S}{E} \text{Re} \left[G_R^*(E, \xi_n, \varphi) F_R(E, \xi_n, -\varphi) e^{i\varphi} \right] \right\}$$
$$\times \left[n(E - eV) - n(E) \right], \quad (30)$$

$$I_{RS}(V) = \frac{e\Gamma_R\Gamma_S}{\pi} \sum_n \int dE N_S(E)$$
$$\times \left\{ |G_R(E, \xi_n, \varphi)|^2 + |F_R(E, \xi_n, \varphi)|^2 \right.$$
$$\left. - \frac{2\Delta_S}{E} \text{Re} \left[G_R(E, \xi_n, \varphi) F_R^*(E, \xi_n, \varphi) e^{i\varphi} \right] \right\}$$
$$\times \left[n(E - eV) - n(E) \right], \quad (31)$$

$$I_{DET}(V) = \frac{e\Gamma_L\Gamma_R}{\pi} \sum_n \int dE |G_R(E, \xi_n)|^2$$

$$\times \left[n(E - eV) - n(E) \right], \quad (32)$$

$$I_{CAR}(V) = \frac{e\Gamma_L\Gamma_R}{\pi} \sum_n \int dE |F_R(E, \xi_n)|^2$$
$$\times \left[n(E - eV) - n(E) \right]. \quad (33)$$

Eqs. (29)-(33) fully determine the currents across the left and the right NS interfaces and represent the central result of our paper.

The current $I_{DET}(V)$ accounts for direct electron transfer between two normal terminals. This current differs from zero also in the normal state of our system. In contrast, $I_{CAR}(V)$ describes the contribution from crossed Andreev reflection which vanishes in the normal limit. The contributions I_{LS} and I_{RS} contain terms which can be interpreted in a similar, though slightly more complicated manner since they originate from the Josephson junction between the superconductors and not from the NS interface. If, just for illustration, we put $\Delta_S = 0$ we immediately get $I_{LS} = (\Gamma_S/\Gamma_R)(I_{DET} + I_{CAR})$ and $I_{RS} = (\Gamma_S/\Gamma_L)(I_{DET} + I_{CAR})$.

We note that the possibility to decompose the currents $I_{L,R}$ into the sum of partial currents (29), each of which depending only on either V_L or V_R (but not on both) is due to the fact that the distribution function in the quantum dot $n_{qd}(E)$ (19) is represented as a linear combination of the distribution functions of the leads. This feature is similar to that of ballistic NSN devices[8,9].

A. Normal state

Let us analyze the above general expressions for the current. Considering first the trivial limit of a normal system $\Delta = \Delta_S = 0$ we obtain

$$n_{qd} = \frac{\Gamma_L n(E + eV_L) + \Gamma_R n(E - eV_R) + \Gamma_S n(E)}{\Gamma_L + \Gamma_R + \Gamma_S}. \quad (34)$$

The current through the left junction is defined by a simple formula

$$I_L = \frac{1}{eR_L} \int dE \left[n_{qd}(E) - n(E + eV_L) \right]. \quad (35)$$

The expression for I_R is similar. Evaluating the integral over E we obtain

$$\begin{pmatrix} I_L \\ I_R \end{pmatrix} = \begin{pmatrix} G_{LL}^N & G_{LR}^N \\ G_{RL}^N & G_{RR}^N \end{pmatrix} \begin{pmatrix} V_L \\ V_R \end{pmatrix} \quad (36)$$

where

$$G_{LL(RR)}^N = \frac{R_S + R_{R(L)}}{R_L R_R + R_L R_S + R_R R_S}, \quad (37)$$

$$G_{LR}^N = G_{RL}^N = \frac{R_S}{R_L R_S + R_R R_S + R_L R_R}. \quad (38)$$

In this limit both local and non-local differential conductances remain voltage-independent.

In the experiments one often measures the non-local resistance

$$R_{LR} = -\left.\frac{\partial V_R}{\partial I_L}\right|_{I_R=0} = \frac{G_{LR}}{G_{LL}G_{RR} - G_{LR}^2}. \quad (39)$$

From Eqs. (36) we obtain

$$R_{LR}^N = R_S. \quad (40)$$

B. Charge imbalance

Charge imbalance[23] is a non-equilibrium phenomenon which is known to cause a number of interesting non-local effects in superconductors. This phenomenon is also of importance in connection with non-local electron transport in NSN hybrid structures discussed here. In particular, it was argued[4,6] that charge imbalance might be responsible for certain features of the non-local conductance observed in experiments. Our approach allows to fully account for this phenomenon and its impact on non-local transport in the system under consideration. In this subsection we briefly illustrate the key physics associated with charge imbalance in our system.

Just for the sake of illustration let us for a moment set $\Delta_S = 0$ and assume $\Gamma_L, \Gamma_R, \Gamma_S \ll \Delta$. In this regime the current I_L (28) across the left junction takes the form[24]

$$I_L = \frac{1}{eR_L}\int dE\, \frac{|E|\theta(|E|-\Delta)}{\sqrt{E^2-\Delta^2}}\left[n(E) - n(E+eV_L)\right]$$
$$+ \frac{1}{eR_L}\int dE\, \theta(|E|-\Delta)\,\tilde{n}_{qd}(E), \quad (41)$$

where $\tilde{n}_{qd}(E)$ is the asymmetric part of the distribution function responsible for charge imbalance[24]. For the system under consideration $\tilde{n}_{qd}(E)$ reads[25]

$$\tilde{n}_{qd}(E) = \frac{\sqrt{E^2-\Delta^2}}{|E|}\frac{n_{qd}(E) + n_{qd}(-E) - 1}{2}, \quad (42)$$

and $n_{qd}(E)$ is given by Eq. (34). Then for local and non-local zero bias conductances one obtains

$$G_{LL(RR)} = \frac{1}{R_{L(R)}}\int dE\, \frac{\theta(|E|-\Delta)}{4T\cosh^2\frac{E}{2T}}\left(\frac{|E|}{\sqrt{E^2-\Delta^2}}\right.$$
$$\left. - \frac{R_{R(L)}R_S}{R_L R_R + R_L R_S + R_R R_S}\frac{\sqrt{E^2-\Delta^2}}{|E|}\right), (43)$$

$$G_{LR} = G_{LR}^N\int dE\, \frac{\theta(|E|-\Delta)}{4T\cosh^2\frac{E}{2T}}\frac{\sqrt{E^2-\Delta^2}}{|E|}. \quad (44)$$

Note that in this regime the non-local conductance is solely due to charge imbalance being fully determined by the second term in Eq. (41). At low temperatures we have $G_{LL}, G_{RR}, G_{LR} \propto e^{-\Delta/T}$. Hence, in the situation considered in this subsection at $T \to 0$ the non-local resistance (39) should diverge as $R_{LR} \propto R_S e^{\Delta/T}$.
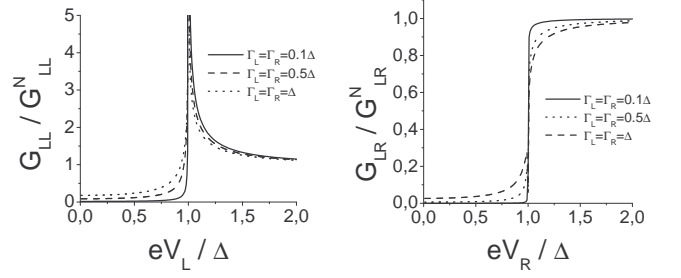

FIG. 2: Normalized local $G_{LL}(V_R)/G_{LL}^N$ and non-local $G_{LR}(V_R)/G_{LR}^N$ differential conductances as a function of applied voltage V_R at low temperature $T \ll \Delta$ and at different tunneling rates $\Gamma_L = \Gamma_R$. Here we set $\Delta_S = \Delta$ and $\Gamma_S = 10\Delta$.
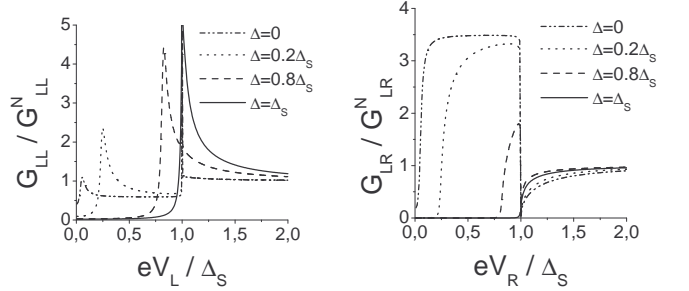

FIG. 3: The same as in Fig. 2 for different values of the dot gap Δ. Here we set $\Gamma_L = \Gamma_R = 0.02\Delta_S$ and $\Gamma_S = 0.1\Delta_S$.

C. General case

Now let us return to the case $\Delta_S \neq 0$. With the aid of Eqs. (32), (33) we determine the differential conductance G_{LR} which is presented in Fig. 2 as a function of applied voltage V_R for $\Delta = \Delta_S$ and different values of the tunneling rates $\Gamma_L = \Gamma_R$ as compared to Δ. We observe that at subgap voltages $eV_R < \Delta$ the magnitude of the normalized non-local conductance G_{LR}/G_N increases with increasing $(\Gamma_L + \Gamma_R)/\Delta$. Such dependence is quite natural because exactly the same ratio controls the strength of the proximity effect in our system. As we have already discussed, with increasing value of the ratio $(\Gamma_L + \Gamma_R)/\Delta$ the proximity-induced subgap electron density of states increases, the difference between DET and CAR contributions grows and, hence, G_{LR} becomes bigger.

Fig. 3 illustrates the effect of the dot order parameter Δ on the non-local conductance. At high voltages $eV_R \gtrsim \Delta_S$ we recover the normal state value (38) while at intermediate values $\Delta \lesssim eV_R \lesssim \Delta_S$ we find $G_{LR} \approx 1/(R_L + R_R)$. For $eV_R < \Delta$ the conductance G_{LR} progressively increases with decreasing ratio Δ/Δ_S and eventually reaches the maximum in the limit $\Delta = 0$ in which case the results[18] are reproduced.

In order to demonstrate an important difference in the low voltage behavior of G_{LR} for superconducting and normal quantum dots in Fig. 3 we deliberately chose small values of tunneling rates $\Gamma_{L,R} \ll \Delta$. We observe

that in the superconducting case G_{LR} essentially vanishes at $eV_R < \Delta$ in accordance with Ref. 7, while for normal quantum dots[18] G_{LR} remains non-zero even at $V_R \to 0$.

V. ZERO-BIAS CONDUCTANCES

Let us now consider the behavior of the conductance matrix in the limit of low voltages in more details. In the zero bias regime currents flowing through the system are low, i.e. we can set $\varphi = 0$. Similarly to Ref. 7 at low voltages the expression for current I_L can be split into three different contributions

$$I_L = G_A V_L + G_{DET}(V_L + V_R) + G_{CAR}(V_L - V_R). \quad (45)$$

Here G_A is (local) Andreev conductance of the left NS barrier, G_{DET} and G_{CAR} are respectively DET and CAR contributions to the zero bias conductance matrix.

A. Zero temperature limit

In the limit of zero temperature $T \to 0$ from Eqs. (29)-(33) we obtain

$$G_A = \frac{e^2}{\pi} \sum_n \frac{2\Gamma_L^2 \left(\Delta^2 + \Gamma_S\Delta + \frac{\Gamma_S^2}{2} \right)}{\left(\xi_n^2 + \Delta^2 + \frac{(\Gamma_L+\Gamma_R)^2 + \Gamma_S^2}{4} + \Gamma_S\Delta \right)^2}, \quad (46)$$

$$G_{DET} = \frac{e^2}{\pi} \sum_n \frac{\Gamma_L\Gamma_R \left(\xi_n^2 + \frac{(\Gamma_L+\Gamma_R)^2}{4} \right)}{\left(\xi_n^2 + \Delta^2 + \frac{(\Gamma_L+\Gamma_R)^2 + \Gamma_S^2}{4} + \Gamma_S\Delta \right)^2}, \quad (47)$$

$$G_{CAR} = \frac{e^2}{\pi} \sum_n \frac{\Gamma_L\Gamma_R \left(\Delta^2 + \Gamma_S\Delta + \frac{\Gamma_S^2}{4} \right)}{\left(\xi_n^2 + \Delta^2 + \frac{(\Gamma_L+\Gamma_R)^2 + \Gamma_S^2}{4} + \Gamma_S\Delta \right)^2}. \quad (48)$$

Let us analyze the above expressions in different physical limits. We first put $\Gamma_S = 0$ and $\Delta = 0$, i.e. we consider a normal quantum dot isolated from the superconducting electrode. Then we obviously find $G_A = G_{CAR} = 0$, while for G_{DET} we obtain

$$G_{DET} = \frac{e^2}{\pi} \sum_n \frac{\Gamma_L\Gamma_R}{\xi_n^2 + \frac{(\Gamma_L+\Gamma_R)^2}{4}}. \quad (49)$$

Comparing this expression to the Landauer formula we immediately conclude that each energy level of the dot effectively corresponds to one conducting channel with transmission

$$\tau_n = \frac{\Gamma_L\Gamma_R}{\xi_n^2 + \frac{(\Gamma_L+\Gamma_R)^2}{4}}. \quad (50)$$

Considering a big metallic quantum dot we can replace the sum over energy states by the integral $\sum_n \to \frac{1}{\delta}\int d\xi$. Making use of the relation between the tunneling rates and the the junction resistances, $\Gamma_{L,R} = \delta/2e^2 R_{L,R}$, we reproduce the standard result

$$G_{DET} = \frac{1}{R_L + R_R}, \quad (51)$$

i.e. in this case DET contribution simply reduces to the Ohm's law.

Next we put $\Gamma_R = 0$ and consider a superconducting dot coupled to one normal and one superconducting lead. In this case one trivially gets $G_{DET} = G_{CAR} = 0$. Provided $\Gamma_L, \Gamma_S \gg \Delta$ the dot can be viewed as a point-like scatterer with the following set of transmission probabilities (cf. Eq. (50))

$$\tilde{\tau}_n = \frac{\Gamma_L\Gamma_S}{\xi_n^2 + \frac{(\Gamma_L+\Gamma_S)^2}{4}}. \quad (52)$$

We note that, although the channel transmissions of NS interfaces remain small, effective transmissions $\tilde{\tau}_n$ are not necessarily small. The Andreev conductance in this limit becomes

$$G_A = \frac{e^2}{2\pi} \sum_n \frac{\Gamma_L^2\Gamma_S^2}{\left(\xi_n^2 + \frac{\Gamma_L^2+\Gamma_S^2}{4} \right)^2}. \quad (53)$$

One can verify that this expression can be cast to the familiar form[21,22]

$$G_A = \frac{e^2}{\pi} \sum_n \frac{2\tilde{\tau}_n^2}{(2 - \tilde{\tau}_n)^2}. \quad (54)$$

In a general case of metallic quantum dots one can perform the summation over ξ_n in Eqs. (46-48) and arrive at the following explicit expressions

$$G_A = \frac{e^2}{4\pi} g_L^2 \frac{\mathcal{B}}{\mathcal{K}^{3/2}}, \quad (55)$$

$$G_{DET} = \frac{e^2}{8\pi} g_L g_R \frac{\mathcal{B} + (g_L + g_R)^2/2}{\mathcal{K}^{3/2}}, \quad (56)$$

$$G_{CAR} = \frac{e^2}{8\pi} g_L g_R \frac{\mathcal{B}}{\mathcal{K}^{3/2}}. \quad (57)$$

where

$$\mathcal{B} = \frac{16\pi^2\Delta^2}{\delta^2} + g_S \frac{4\pi\Delta}{\delta} + \frac{g_S^2}{4} \quad (58)$$

and

$$\mathcal{K} = \frac{16\pi^2\Delta^2}{\delta^2} + \frac{(g_L + g_R)^2 + g_S^2}{4} + g_S \frac{4\pi\Delta}{\delta}. \quad (59)$$

In the limit $\Delta \to 0$ our results for G_{DET} and G_{CAR} reduce to the corresponding expressions derived in Ref.

18 for the normal quantum dot. At the same time, our result (55) for the Andreev conductance G_A (for $\Delta \to 0$) turns out to be 4 times bigger than the analogous expression[18]. This difference is supposed to be due to a different definition of the Andreev conductance employed in Ref. 18.

Combining the above results for G_{DET} and G_{CAR} we immediately arrive at the zero temperature linear non-local conductance $G_{LR} = G_{DET} - G_{CAR}$ for our device. It reads

$$G_{LR} = \frac{e^2}{16\pi} \frac{g_L g_R (g_L + g_R)^2}{\left(\frac{16\pi^2 \Delta^2}{\delta^2} + \frac{(g_L+g_R)^2+g_S^2}{4} + g_S \frac{4\pi\Delta}{\delta} \right)^{3/2}}. \quad (60)$$

This expression demonstrates again why the lowest order perturbation theory in barrier transmissions[7] yields zero non-local conductance at $T = 0$. This perturbation theory applies in the weak tunneling limit $g_{L,R} \ll 1$. The result (60), however, contains only higher order terms in barrier transmissions whereas the contribution $\propto g_L g_R$ should vanish. This situation is qualitatively similar to that of NSN structures with ballistic electrodes[8,9]. We would also like to emphasize that the exact cancellation of G_{DET} and G_{CAR} in the lowest order in $g_L g_R$ holds for any g_S and *does not* require taking the limit $g_S \to \infty$. This is in contrast to the case of normal quantum dots[18] in which G_{LR} was found to vanish *only* for $g_S \to \infty$.

At small tunneling rates $\Gamma_L, \Gamma_R, \Gamma_S \ll \Delta$ Eq. (60) reduces to

$$G_{LR} = \frac{e^2}{(16\pi)^4} \frac{g_L g_R (g_L + g_R)^2 \delta^3}{\Delta^3}. \quad (61)$$

In the limit of a bulk metal $\delta \to 0$ (though $d \lesssim \xi_0$) the proximity effect becomes unimportant and the non-local conductance G_{LR} (61) vanishes already to *all* orders in $g_{L,R}$.

Finally, we present the exact expression for the zero temperature non-local resistance R_{LR}. It reads

$$\frac{R_{LR}}{R_S} = \frac{2\Gamma_S \left(\left(\Delta + \frac{\Gamma_S}{2}\right)^2 + \frac{(\Gamma_L+\Gamma_R)^2}{4} \right)^{3/2}}{\left(2\left(\Delta + \frac{\Gamma_S}{2}\right)^2 + \frac{(\Gamma_L+\Gamma_R)^2}{4} \right)^2 - (\Gamma_L+\Gamma_R)^2}. \quad (62)$$

In the limit $\Gamma_S \gg \Delta, \Gamma_L, \Gamma_R$ we get $R_{LR} = R_S$, i.e. in this limit the non-local resistance just coincides with its normal state value. For $\Delta \gg \Gamma_L, \Gamma_R, \Gamma_S$ we obtain $R_{LR} = \delta/4e^2\Delta \ll R_S$.

B. Non-zero temperatures

Finally let us briefly discuss the effect of temperature on zero bias conductances of our system. Combining Eqs. (29)-(33) and (45) we obtain

$$G_{LL} = \frac{e^2 \Gamma_L \Gamma_S}{\pi} \sum_n \int dE \frac{|E|\theta(|E| - \Delta_S)}{\sqrt{E^2 - \Delta_S^2}}$$
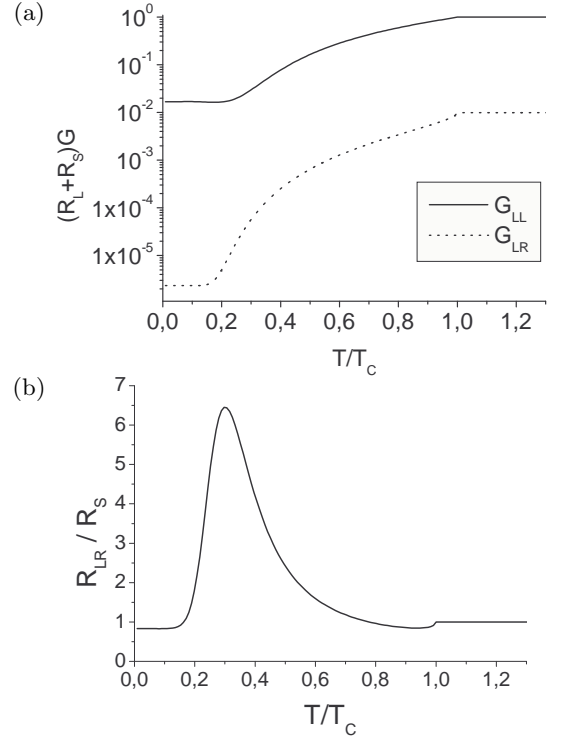

(a)

(b)

FIG. 4: (a) temperature dependence of local G_{LL} (63) and non-local G_{LR} (64) zero-bias conductances. The parameters were chosen as follows: $\Delta = \Delta_S$, $\Gamma_L = \Gamma_R = 0.1\Delta(0)$, $\Gamma_S = 10\Delta(0)$; (b) non-local zero bias resistance R_{LR} (39) normalized by its normal state value (for the same parameters).

$$\times \frac{1}{4T\cosh^2(E/2T)} \left\{ |G_R(E,\xi_n)|^2 + |F_R(E,\xi_n)|^2 \right.$$
$$\left. - \frac{2\Delta_S}{E} \text{Re}\left[G_R(E,\xi_n)F_R^*(E,\xi_n) \right] \right\}$$
$$+ \frac{e^2\Gamma_L\Gamma_R}{\pi} \sum_n \int \frac{dE}{4T\cosh^2(E/2T)}$$
$$\times \left\{ |G_R(E,\xi_n)|^2 + \left(\frac{2\Gamma_L}{\Gamma_R} + 1 \right) |F_R(E,\xi_n)|^2 \right\}, \quad (63)$$

$$G_{LR} = \frac{e^2\Gamma_L\Gamma_R}{\pi} \sum_n \int dE \frac{|G_R(E,\xi_n)|^2 - |F_R(E,\xi_n)|^2}{4T\cosh^2(E/2T)} \quad (64)$$

Substituting the expressions for the Green functions (23)-(25) into the above equations we arrive at the final results for zero-bias conductances at non-zero T. These results are illustrated in Figs.4 and 5.

Fig. 4 shows the temperature dependence of both local and non-local zero bias conductances (63), (64) along with that for the non-local resistance (39). The conductances G_{LL} and G_{LR} decrease monotonously with decreasing temperature. The temperature dependence of the non-local resistance R_{LR} is, on the contrary, non-monotonous. At temperatures just below T_C the resistance R_{LR} first slightly decreases but then it starts
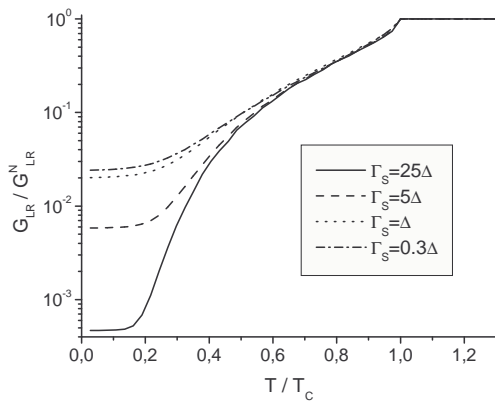
FIG. 5: Temperature dependence of zero-bias non-local conductance G_{LR} for different values of Γ_S. Here we set $\Delta = \Delta_S$, $\Gamma_L = \Gamma_R = 0.3\Delta(0)$.

growing exponentially with decreasing T due to charge imbalance effects, as it was explained in Sec. 3b. Such a tendency persists down to the crossover temperature

$$T^* \sim \frac{\Delta}{\ln \frac{2\Delta + \Gamma_S}{\Gamma_L + \Gamma_R}}, \quad \Gamma_L, \Gamma_R \ll 2\Delta + \Gamma_S \qquad (65)$$

at which the non-local resistance reaches its maximum. Below T^*, AR contribution starts dominating over that caused by charge imbalance. For this reason at $T < T^*$ R_{LR} drops sharply and then at $T \sim T^*/2$ saturates to its zero temperature value (62), as it is seen in Fig. 4.

Note that qualitatively the same behavior of the non-local resistance was recently observed in experiments[4,6], cf., eg., Fig. 3 in Ref. 6. Though a detailed quantitative comparison between our theoretical predictions and the experimental results[4,6] is rather difficult to perform due to different geometry of the model employed here, we believe that our theory correctly describes the physical origin of the peak in the temperature dependence of the non-local resistance observed in Refs. 4,6.

For completeness, in Fig. 5 we present the dependence $G_{LR}(T)$ at different values of Γ_S. As temperature decreases below the critical temperature T_C the conductance $G_{LR}(T)$ drops sharply below its normal state value (38) and at $T \ll T_C$ it saturates to the zero-temperature value which essentially depends of the relation between $\Gamma_{L,R,S}$ and Δ. We observe that for given $\Gamma_{L,R}$ this value *decreases* with increasing coupling Γ_S between the dot and the superconducting lead. This tendency is explained by the fact that CAR becomes progressively more pronounced with increasing tunneling rate Γ_S.

VI. CONCLUSIONS

In this paper we developed a microscopic theory of non-local electron transport in three-terminal NSN structures which consist of a superconducting chaotic quantum dot (with typical size $d \lesssim \xi_0$) attached to one superconducting and two normal reservoirs, as it is shown in Fig. 1. By varying the tunneling rates between the dot and the electrodes $\Gamma_{L,R,S}$ (which play the role of effective Thouless energies for electrons in the part of a superconducting electrode directly attached to normal leads) one can cover a number of different physical situations and limits and illustrate the relation to the models considered by other authors.

Our analysis is employed within the general Keldysh formalism which fully accounts for non-equilibrium effects and disorder in the superconducting terminal (dot). Our theory allows to go beyond perturbation theory in dimensionless conductances between S- and N-electrodes $g_{L,R}$ and derive a general expression for the conductance matrix which remains valid in both weak and strong tunneling limits. This result enables one to study and compare relative contributions to the non-local conductance provided by the competing processes of direct electron transfer (DET) and crossed Andreev reflection (CAR). We demonstrated that at low energies these contributions do not cancel each other beyond the weak tunneling limit. This is the result of the proximity effect: Coupling to normal electrodes yields non-zero subgap density of states inside the superconducting dot which in turn causes a decrease of the CAR contribution to the non-local conductance G_{LR}. On the contrary, increasing coupling between the dot and the superconducting electrode increases CAR and, hence, decreases G_{LR}.

Our theory allows to investigate the effect of charge imbalance on non-local electron transport in NSN devices. We argued that temperature dependence of the non-local resistance R_{LR} of such devices is determined by the competition between charge imbalance and Andreev reflection. The contribution of the former process dominates over that of the latter at $T \gtrsim T^*$ (where T^* is the crossover temperature defined in Eq. (65)) causing an increase $R_{LR}(T)$ with decreasing T. In contrast, at lower temperatures AR dominates and $R_{LR}(T)$ decreases as T becomes lower. As a result, the dependence $R_{LR}(T)$ acquires a pronounced peak at $T \sim T^*$, see Fig. 4. This behavior was observed in recent experiments[4,6].

[1] J.M. Byers and M.E. Flatte, Phys. Rev. Lett. **74**, 306 (1995).

[2] G. Deutscher and D. Feinberg, Appl. Phys. Lett. **76**, 487 (2000).

[3] A.F. Andreev, Zh. Eksp. Teor. Fiz. **46**, 1823 (1964) [Sov. Phys. JETP **19**, 1228 (1964)].

[4] D. Beckmann, H.B. Weber, and H. v. Löhneysen, Phys. Rev. Lett. **93**, 197003 (2004); D. Beckmann and H. v. Löhneysen, cond-mat/0609766.

[5] S. Russo, M. Kroug, T.M. Klapwijk, and A.F. Morpurgo, Phys. Rev. Lett. **95**, 027002 (2005).

[6] P. Cadden-Zimansky and V. Chandrasekhar, Phys. Rev. Lett. **97**, 237003 (2006) .

[7] G. Falci, D. Feinberg, and F.W.J. Hekking, Europhys. Lett. **54**, 255 (2001).

[8] M.S. Kalenkov and A.D. Zaikin, Phys. Rev. B **75**, 172503 (2007).

[9] M.S. Kalenkov and A.D. Zaikin, cond-mat/07063575.

[10] T. Yamashita, S. Takahashi, and S. Maekawa, Phys. Rev. B **68**, 174504 (2003).

[11] R. Melin and D. Feinberg, Phys. Rev. B **70**, 174509 (2004).

[12] F. Giazotto, F. Taddei, F. Beltram, and R. Fazio, Phys. Rev. Lett. **97**, 087001 (2006).

[13] A. Levy Yeyati, F.S. Bergeret, A. Martin-Rodero, and T.M. Klapwijk, Nature Physics **3**, 455 (2007).

[14] A.D. Zaikin, Phyica B **203**, 255 (1994).

[15] A. Huck, F.W.J. Hekking, and B. Kramer, Europhys. Lett. **41**, 201 (1998).

[16] A.V. Galaktionov and A.D. Zaikin, Phys. Rev. B **73**, 184522 (2006).

[17] A. Brinkman and A.A. Golubov, Phys. Rev. B **74**, 214512 (2006).

[18] J.P. Morten, A. Brataas, and W. Belzig, Phys. Rev. B **74**, 214510 (2006).

[19] S. Duhot and R. Melin, Phys. Rev. B **75**, 184531 (2007).

[20] I.L. Aleiner, P.W. Brouwer, and L.I. Glazman, Phys. Rep. **358**, 309 (2002).

[21] G.E. Blonder, M. Tinkham, and T.M. Klapwijk, Phys. Rev. B **25**, 4515 (1982).

[22] C.W.J. Beenakker, Rev. Mod. Phys. **69**, 731 (1997).

[23] M. Tinkham and J. Clarke, Phys. Rev. Lett. **28**, 1366 (1972).

[24] M. Tinkham, Phys. Rev. B **6**, 1747 (1972).

[25] D.S. Golubev and A. Vasenko, in: *International Workshop on Superconducting Nano-Electronics Devices*, ed. by J.P. Pekola, B. Ruggiero, and P. Silverstrini (Kluwer Academic/Plenum, New York), p. 165 (2002).